PHYSICAL REVIEW B VOLUME 35, NUMBER 10 1 APRIL 1987

Three-body correlations in liquid and solid ^{4}He

P. A. Whitlock
Courant Institute of Mathematical Sciences, New York University, New York, New York 10012

G. V. Chester
Laboratory of Atomic and Solid State Physics, Cornell University, Ithaca, New York 14853
(Received 15 August 1986; revised manuscript received 3 December 1986)

We present the analysis of three-body correlations in the fluid and solid phases of ^{4}He. The results are from exact (Green's-function Monte Carlo) and variational calculations of ^{4}He described by the Lennard-Jones two-body potential. A set of angular order parameters derived from the three-body distribution function are defined and we find that certain of these parameters change significantly at the onset of freezing to a quantum solid. We then trace the evolution of the parameters from the quantum solid regime, near melting, to an approximately harmonic solid at high density. We have also computed the angular order parameters for two different kinds of variational functions: the traditional Jastrow function and a function which includes triplet correlations. The parameters computed from the Jastrow function show clear differences from the exact results. The variational function with triplet correlations, however, closely resembles the exact results in both the fluid and solid phases. In this respect it is clearly superior to the Jastrow function.

I. INTRODUCTION

It is well known that the spatial order in both liquid and solid helium is very different from that found in simple classical fluids and solids such as liquid and solid argon. The quantum phases are of course weakly bound, the positive kinetic energy being of the same magnitude as the negative potential energy. The spatial correlations, as revealed in the structure function and pair correlation function, are very weak. This lack of structure is particularly noticeable in the fluid phase just before freezing. The main purpose of this paper is to look in more detail at the structure in both the fluid and solid phases. In particular we present detailed data, based on three-body correlations, on the evolution of the spatial order as the system freezes. Similarly, we show the development of the spatial order from a low-density quantum solid to an approximately harmonic solid at much higher density. Most of our data have been generated by exact quantum-mechanical computer simulations of the liquid and solid phases of ^{4}He. We also thought it worthwhile to compare these with corresponding data obtained from variational wave functions.

Two general features of the melting and freezing of a simple classical system are now well established. First, the transition between the fluid and solid phases is dominated by entropy changes.[1] This is clearly seen from the melting and freezing transition of the hard-sphere system which is entirely entropic. It is now well established that the hard-sphere transition provides a good model for the transition in other central-force systems.[2] Second, a very strong precursor of the freezing transition is found in simple fluids.[3] The intermediate-range spatial correlations build up in the pair distribution function. Since the transition is first order, the spatial correlations build up but then saturate, leading to a large but finite first peak in $S(k)$. For a wide range of central-force fluids the first peak in $S(k)$ reaches a height of 2.85 along the freezing line.[3] This value for the first peak of $S(k)$ has also been found in experimental studies in liquid argon.[4]

The two quantum systems, ^{4}He and ^{3}He, undergo melting and freezing in a very different fashion from that described above. First, we point our that the melting and freezing transitions at absolute zero cannot, by Nernst's law, involve entropy changes. The transition must be driven by energy changes. In this respect the quantum transition is fundamentally different from the classical transition. Second, the solid phase of these quantum systems, near melting, is completely different in character from a classical solid. The quantum solids have a very low density, and extremely large zero-point oscillations of the atoms on the lattice.[5] They are unique in that their kinetic and potential energies are of comparable magnitude.[6] The very large zero-point energies of these light and weakly bound systems lead to a new type of solid which has no counterpart in classical physics. Third, no precursor for freezing has yet been found in these systems. The particles are very weakly correlated in the fluid phase, while the first peak of the structure factor, at freezing, reaches a value of 1.5 in ^{4}He (Ref. 6) and $g(r)$ evolves smoothly as the freezing transition is approached.

It was these considerations that led us to look in more detail at the local order in the fluid and solid phases of ^{4}He. The methods we have adopted are derived from the work of Chui and Williams[7] in their study of the classical Lennard-Jones (LJ) fluid and solid.[8]

Chui and Williams proposed a particularly useful way of presenting the information contained in the triplet correlation function $g_3(r_{12},r_{13},r_{23})$. A local coordinate system is defined with its z axis along the vector between

a particle and its nearest neighbor; r and Ω are then measured with respect to this coordinate system. A spherical harmonic analysis is made, and this expansion leads to a set of angular order parameters $g_{l,m}(r)$ each of which is a function of distance r. They contain the basic information about the local angular order in the fluid and solid phases. Our presentation of the detailed data describing these order parameters for the fluid and solid phase of ^{4}He is a first attempt to understand in more detail higher spatial correlations in both phases. It is unfortunately true that when one passes beyond the level of two-body correlations, presentation of results becomes a major task. We have thought it worthwhile to present a comprehensive set of data so that readers may be stimulated to make new comparisons and perhaps obtain new insights into the behavior of the system at the microscopic level.

In this paper we present the results of exact and variational computations for a range of $g_{l,m}(r)$'s for both the fluid and solid phases of ^{4}He. We find that certain of these angular order parameters change significantly at the onset of freezing to a quantum solid. We have also computed these order parameters at three densities in the solid phase. At the highest of these densities, $\rho\sigma^3=1.1$, the solid has become approximately harmonic. We are thus able to trace the evolution of these functions as we move from the quantum solid regime near melting to an approximately harmonic solid at high density.

Finally we have computed these functions for two different kinds of variational functions: the traditional Jastrow function and a function which includes triplet correlations. The order parameters computed from the Jastrow function show some clear differences from the exact results. The variational function with triplet correlations, however, almost exactly reproduces the results in both the fluid and solid phases. In this respect it is clearly superior to the Jastrow function. It is significant, although not altogether surprising, that explicit use of triplet correlations can improve agreement with exact results.

In Sec. II we will define the angular order parameters and discuss how they were computed for the fluid and solid phases. Section III is devoted to a discussion of the pair distribution function for ^{4}He. In Sec. IV we discuss the behavior of the angular order parameters as the system freezes. Section V deals with the evolution of $g_{l,m}(r)$ from low to high density in the solid phase, while Sec. VI is devoted to our results using variational wave functions. Our conclusions are presented in Sec. VII.

II. METHOD

The angular order parameters, $g_{l,m}(r)$ are defined by

$$g_{l,m}(r)=\sqrt{4\pi}\int g_3(r,\Omega)Y_{l,m}(\Omega)d\Omega\ , \tag{1}$$

where $g_3(r,\Omega)$ is a restricted three-particle distribution function given by the equation

$$g_3(r_{13},\Omega)=\rho^{1/3}\int_{r_{12}<r_{13}}dr_{12}\left[g_3(r_{12},r_{13},r_{23})-\rho\int_{r_{14}<r_{12}}g_4(r_{12},r_{13},r_{23},\mathbf{r}_4)d\mathbf{r}_4\right]\ . \tag{2}$$

Three-particle configurations can always be described by the lengths of the sides of the triangle with particles at the vertices. In Eq. (2), we have denoted these lengths by r_{12}, r_{13}, and r_{23}. The quantity r_{12} is defined to be the distance of the nearest neighbor from particle 1. Particle 3 is at a distance r_{13} and in a direction given by the angle Ω. The vector $\mathbf{r}_{12}$ provides a polar axis to define this angular direction. The integral over the four-particle distribution function, $g_4(r_{12},r_{13},r_{23},\mathbf{r}_4)$, gives the probability of finding a fourth particle nearer to particle 1 than particle 2. Hence, when this quantity is subtracted from $g_3(r_{12},r_{13},r_{23})$, we are left with a restricted three-particle distribution function that insures that no fourth particle is closer to particle 1 than particle 2. The final integration over the distance r_{12} ensures that the calculation is carried out for all values of the nearest-neighbor distance r_{12} which by definition must be less than r_{13}.

Equation (2) provides a formal definition of $g_3(r,\Omega)$ in terms of the basic correlation functions $g_3(r_{12},r_{13},r_{23})$ and $g_4(r_{12},r_{13},r_{23},\mathbf{r}_4)$. In principle this function could be computed from Eq. (2) by inserting the appropriate value of $g_3(r_{12},r_{13},r_{23})$ and $g_4(r_{12},r_{13},r_{23},\mathbf{r}_4)$. We have, however, found it more convenient to compute $g_3(r,\Omega)$ directly from the configurations of the particles. We start by defining a local coordinate system for each particle. The line from particle i to its nearest neighbor defines the z axis. The y axis then lies in the plane defined by particle i and its two nearest neighbors. Finally, the x axis is chosen perpendicular to the y and z axes. The interparticle distance, r, is that between particles i and j, where j is any particle in the system other than the nearest neighbor to i. The solid angle Ω is measured with respect to this coordinate system.[9]

Upon referring to Eq. (1), it is apparent that the $g_{l,m}(r)$ will vary in sign and as r becomes large, the asymptotic value will be zero. If the particles in the fluid are arranged completely randomly, even at small values of r, the $g_{l,m}(r)$ will be just noisy fluctuations about zero. Due to the weighting of the spherical harmonics, the $g_{l,m}(r)$ are sensitive to even minor angular orderings in the fluid and several interesting phenomena have been observed with them. In the solid, where there is well defined local angular order, the $g_{l,m}(r)$ are an appropriate tool to describe it.

The values of $g_{l,m}(r)$ were determined for $l=2$, 4, and 6 and $m=0,1,\ldots,l$. The imaginary components of $g_{l,m}(r)$ were found to be equal to zero on the average. The overall isotropy of the fluid implies that the $g_{l,m}(r)$ with l odd will vanish and our simulations verified this conclusion. No interesting phenomena were observed in

$g_{2,m}(r)$ and they will not be discussed further.

The calculations were carried out for the liquid and solid phases of the quantum Lennard-Jones system. The Green's-function Monte Carlo (GFMC) and variational calculations produce sets of particle coordinates (which we call configurations) whose distributions reflect the wave functions. In particular, the particle configurations were taken from GFMC simulations and variational calculations of ^{4}He with the LJ potential at absolute zero. GFMC is a method for solving the Schrödinger equation subject only to statistical sampling errors. Whitlock *et al.*[6] used such GFMC configurations to determine the equation of state, radial distribution function, structure function, momentum distribution and other properties of the LJ ^{4}He system.

For each density studied in the quantum liquid, on the order of 4000 GFMC particle configurations were analyzed. In the solid, and for the variational calculations, approximately 2000 configurations were analyzed at each density. In the regions of interest, the statistical errors in $g_{l,m}(r)$ vary from 2–10%. At the peaks, the errors are usually at the low end of the range.

III. BEHAVIOR OF THE PAIR CORRELATION FUNCTION

In Sec. II we defined a set of angular correlation functions $g_{l,m}(r)$ as angular averages of the three-particle correlation function. We will see that these functions oscillate about zero and in most cases die away fairly quickly as r increases. In this section we will discuss the behavior of the correlation function $h(r)$ defined in the usual way as

$$h(r)=g(r)-1 \ .$$

This function also oscillates about zero and tells us how the spherical average of the two-particle correlations behave. We should point our that in the solid phase, $h(r)$ will show oscillations about zero for very large r. This merely reflects the fact that there is long-range order in a three-dimensional quantum solid.

In Fig. 1, we show $h(r)$ for three densities, namely, $\rho\sigma^3=0.365$, 0.490, and 0.526. The first is the equilibrium fluid at zero pressure, the second a high-density metastable fluid, while the highest density is a crystal just above melting.[10] The figure shows that $h(r)$, and hence $g(r)$, evolves smoothly from the lowest-density fluid to the crystal phase. The amplitude of the oscillations grow but there is no qualitative difference between $h(r)$ in the fluid and in the low-density crystal. Indeed $h(r)$ in the low-density crystal is remarkably fluid like in its appearance. This is in striking contrast to the behavior of $h(r)$ in a classical crystal just above the melting line.[11] It is worth emphasing that in a dense classical fluid near freezing, $h(r)$ shows much more intermediate range structure. The height of the second peak of $h(r)$ is 0.3 in the dense classical fluid just before freezing.[12] In the metastable fluid phase of ^{4}He, on the other hand, the second peak of $h(r)$ is only 0.1.

Figure 2 shows the evolution of $h(r)$ as the density is increased from the metastable fluid ($\rho\sigma^3=0.490$) to a very dense crystal ($\rho\sigma^3=1.1$). Even at a density of $\rho\sigma^3=0.622$, which is 25% above the melting density, the shape of $h(r)$ is very close to that in the dense fluid. Only when a very high density ($\rho\sigma^3=1.1$) is reached does a qualitative change appear. At this density, new structure is apparent in $h(r)$—it is very close to that in a classical crystal near melting.[11] The solid has now become much more harmonic and much more highly correlated. The root-mean-square displacement of the particles from their sites is only 0.13 of the interparticle spacing, rather close to that of a classical solid near melting. In contrast, the ratio is 0.30 for the quantum solid near freezing with $\rho\sigma^3=0.526$.

We can summarize the behavior of $h(r)$ by saying that it maintains a smooth fluid like shape from the low-density fluid well into the crystal phase. Only at a very high density does new structure appear. Thus the pair distribution function is highly insensitive to the freezing transition. We will see in the subsequent sections of this paper that several of the $g_{l,m}(r)$ behave in a strikingly different fashion.

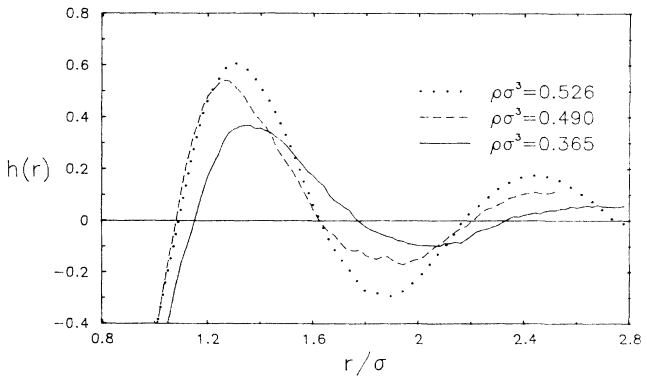

FIG. 1. Comparison of $h(r)$, the direct correlation function, from an exact (GFMC) calculation for the Lennard-Jones ^{4}He system at two densities in the liquid, $\rho\sigma^3=0.365$, 0.490, and one solid density, $\rho\sigma^3=0.526$.

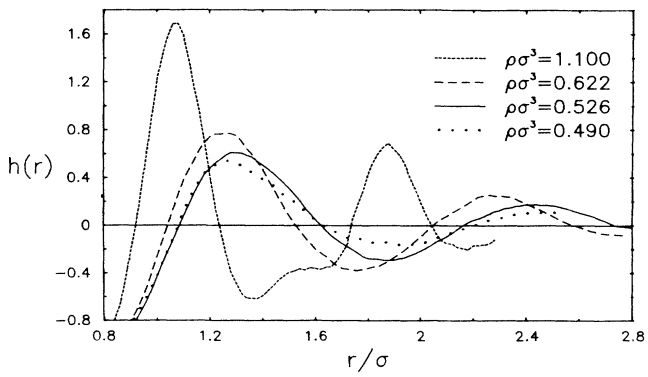

FIG. 2. Comparison of the calculated $h(r)$ for the Lennard-Jones ^{4}He system at three solid densities, $\rho\sigma^3=0.526$, 0.622, 1.100, and a dense metastable liquid density, $\rho\sigma^3=0.490$. The $h(r)$ at $1.10\sigma^{-3}$ is from a variational calculation. The rest are from GFMC calculations.

IV. CHANGE IN ANGULAR ORDER AS THE SYSTEM FREEZES

In this section we present the results from our exact computations of the angular order parameters, $g_{l,m}(r)$. We compare the form of these functions in the lowest-density fluid ($\rho\sigma^3=0.365$), the high-density fluid ($\rho\sigma^3=0.490$), and the solid near its melting density ($\rho\sigma=0.526$). In Fig. 3(a) and 3(b) we show the parameters with $l=4$ and 6 for the lowest-density fluid. There is clearly a great deal of information in these functions. However our focus here is on the behavior of these order parameters as the fluid freezes. In Fig. 4(a) and 4(b) we show the same parameters in the solid at the density $\rho\sigma^3=0.526$, which is near the melting density of the solid. A careful comparison of Fig. 3 and 4 reveals that only $g_{4,3}$, $g_{6,1}$, $g_{6,2}$, and $g_{6,5}$ show qualitative changes between fluid and solid. The remaining functions change in a way consistent with an increase in the density, that is, the amplitudes increase and the peaks grow narrower. We now give a more detailed discussion of the four functions thus singled out.

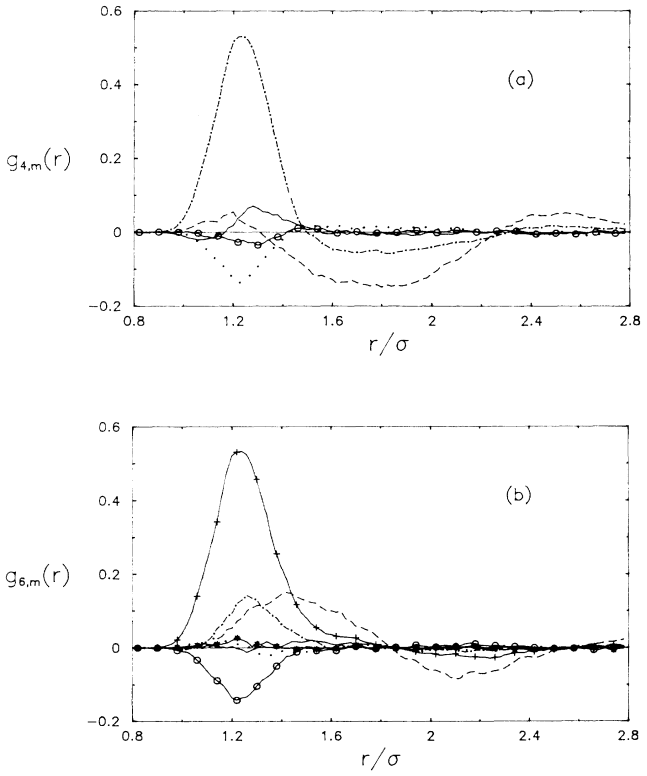

FIG. 3. (a) $g_{4,m}(r)$ for the equilibrium liquid, $\rho\sigma^3=0.365$, derived from a GFMC calculation. The individual curves are identified as follows: — — —, $g_{4,0}(r)$; · · · ·, $g_{4,1}(r)$; ——, $g_{4,2}(r)$; -○-○-, $g_{4,3}(r)$; and —·—·—·, $g_{4,4}(r)$. (b) $g_{6,m}(r)$ for the equilibrium liquid, $\rho\sigma^3=0.365$, derived from a GFMC calculation. The individual curves are identified as follows: — — —, $g_{6,0}(r)$; · · · ·, $g_{6,1}(r)$; ——, $g_{6,2}(r)$; -○-○-, $g_{6,3}(r)$; —·—·—·, $g_{6,4}(r)$; -*-*-, $g_{6,5}(r)$; and - + - + -, $g_{6,6}(r)$.

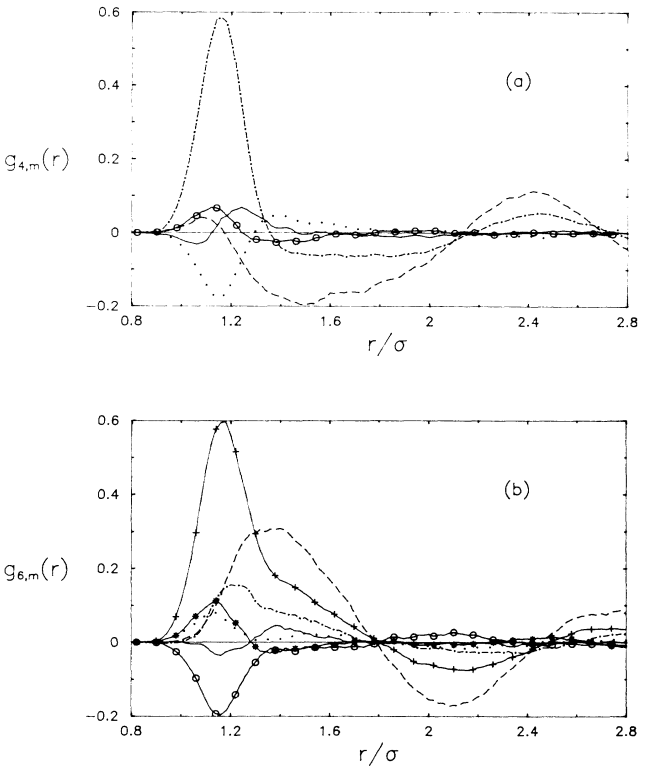

FIG. 4. (a) $g_{4,m}(r)$ for a low-density solid, $\rho\sigma^3=0.526$, derived from a GFMC calculation. The identification of the individual curves is the same as in Fig. 3(a). (b) $g_{6,m}(r)$ for a low-density solid, $\rho\sigma^3=0.526$, derived from a GFMC calculation. The identification of the individual curves is the same as in Fig. 3(b).

For $l=4$ we concentrate on $g_{4,3}$. Figure 5 shows the function for three densities. As the density is increased from the equilibrium value, $\rho\sigma^3=0.365$, to the high density metastable fluid, $\rho\sigma^3=0.490$, almost no significant change occurs. The most noticeable change is that a small positive peak occurs at $r=\sigma$ in the metastable fluid.

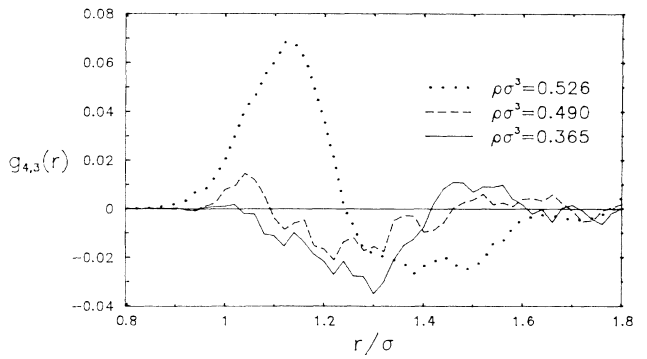

FIG. 5. Comparison of $g_{4,3}(r)$ as the LJ ^{4}He freezes. Two densities are in the liquid, viz., $\rho\sigma^3=0.365$, 0.490, and one is in the solid phase, $\rho\sigma^3=0.526$.

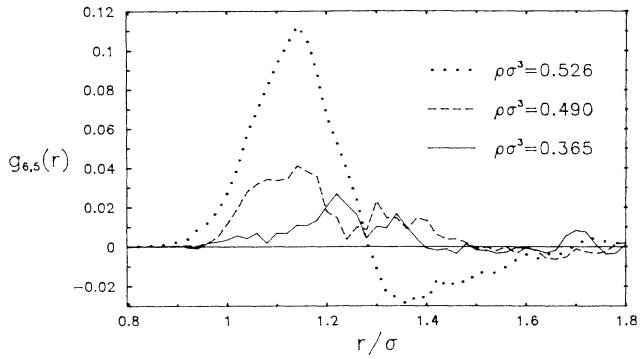

FIG. 6. Comparison of $g_{6,5}(r)$ as the LJ ^{4}He system freezes. Two densities are in the liquid, viz., $\rho\sigma^3=0.365$, 0.490, and one is in the solid phase, $\rho\sigma^3=0.526$.

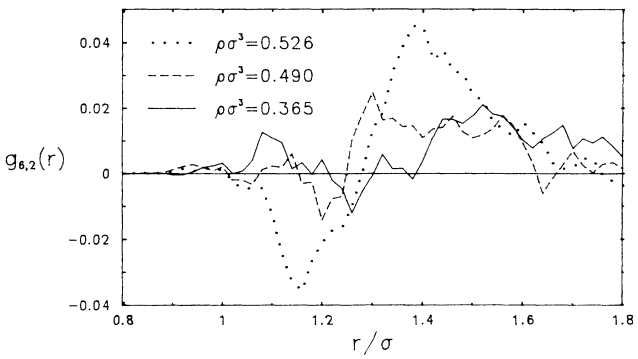

FIG. 8. Comparison of $g_{6,2}(r)$ as the LJ ^{4}He system passes through a phase transition.

However as the system freezes, $g_{4,3}$ suddenly acquires a large positive peak, close to $r=\sigma$. The change is dramatic. There is only a 6% change in density between the metastable fluid state and the solid near freezing. This small increase in density produces an increase in height of the peak by a factor of 12. This is to be contrasted with an almost negligible change in the entire fluid range in which there was a 30% increase in density.

For $l=6$, we first examine $g_{6,5}$, whose behavior is shown in Fig. 6. This function also shows a dramatic change at freezing. The function $g_{6,5}$ is small and positive in the fluid phase for most values of r. As the system freezes it acquires a large positive first peak near $r=\sigma$, and develops a moderate negative peak at $r=1.4\sigma$. The metastable fluid shows no significant precursor for this behavior.

Figure 7 shows the same comparisons for $g_{6,1}$. For this function the behavior is not as dramatic as we found for $g_{6,5}$. However the function becomes entirely positive on freezing and the first peak doubles in height.

The same comparisons for $g_{6,2}$ are shown in Fig. 8. In the solid phase the function $g_{6,2}$ undergoes a complete oscillation from negative to positive values between $r=\sigma$ and $r=1.5\sigma$. The metastable fluid shows a very weak precursor for this behavior while in the equilibrium fluid, $g_{6,2}$ is small and positive through most of this range.

We can summarize these results as follows. First, none of the $g_{l,m}(r)$ changes very much as the fluid is compressed from low density to the high-density metastable regime. On the other hand, four of these functions undergo significant changes when we move from the high-density fluid to the solid phase. For these four order parameters the angular order in the solid is quite different from that in the dense fluid. However no significant precursors for this behavior are found in the fluid phase. Finally we note that apart from these four order parameters, the remaining functions are similar in the high-density fluid and the low-density solid. In other words, most of $g_{l,m}(r)$ in the quantum solid are remarkably close to those in the fluid phase. In the next section we will see that this is characteristic of a quantum solid. In the high-density ^{4}He solid, which is approximately harmonic, several of the $g_{l,m}(r)$ show very much more structure than in the quantum solid near melting.

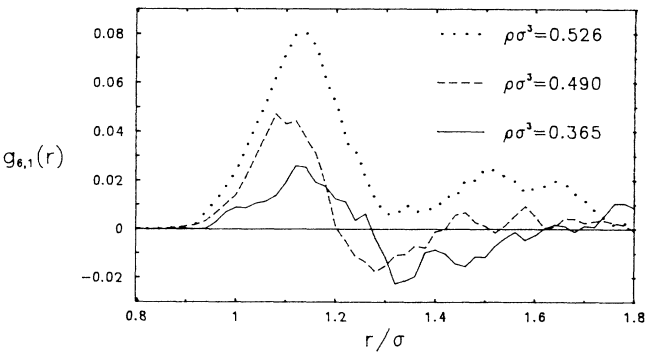

FIG. 7. Comparison of $g_{6,1}(r)$ as the LJ ^{4}He system freezes. Two densities are in the liquid, viz., $\rho\sigma^3=0.365$, 0.490, and one density is in the solid phase, $\rho\sigma^3=0.526$.

V. ANGULAR ORDER IN THE SOLID PHASE

We have computed the angular order parameters for $l=4$ and $l=6$ at three densities in the solid phase, namely, $\rho\sigma^3=0.526$, 0.622, and 1.1. At the two lower densities the computations were made using the exact GFMC method. At the highest density we have carried out only variational calculations. However at this high density the solid is approximately harmonic and we therefore believe that there will be little difference between the variational and exact results. At the highest density the ratio of the root-mean-square displacement of the particles from their lattice sites to the near-neighbor distance—Lindeman's ratio—is 0.13. This value for the ratio may be compared with the value in a classical solid near melting, namely, 0.15–0.17. This comparison suggests that our high-density solid helium is somewhat more harmonic than a classical solid near melting. It is clearly much more harmonic than a quantum solid near melting, where Lindeman's ratio is approximately 0.30.

In Figs. 9(a) and 9(b), we show $g_{4,m}$ and $g_{6,m}$ at

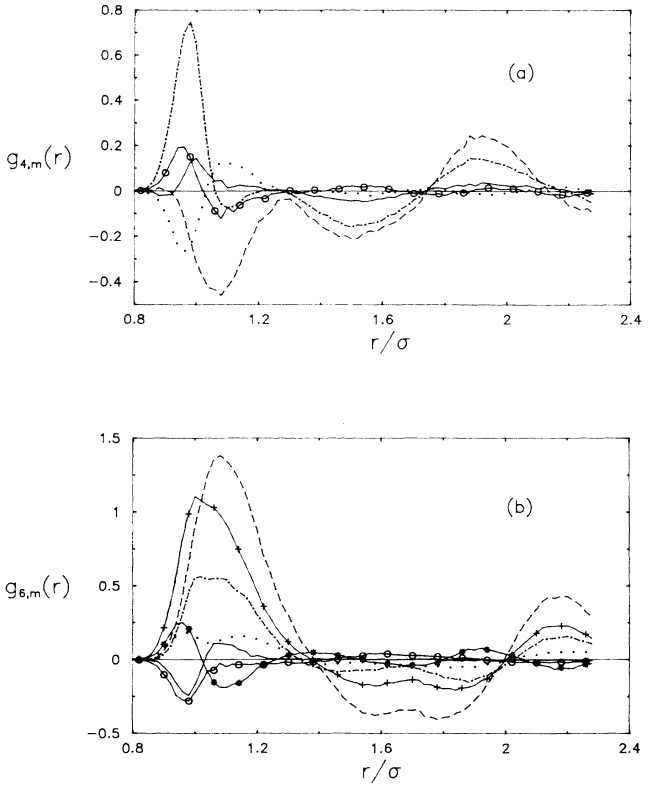

FIG. 9. (a) $g_{4,m}(r)$ for a high-density solid, $\rho\sigma^3=1.10$, derived from a variational calculation. The identification of the individual curves is the same as in Fig. 3(a). (b) $g_{6,m}(r)$ for a high-density solid, $\rho\sigma^3=1.10$, derived from a variational calculation. The identification of the individual curves is the same as in Fig. 3(b).

$\rho\sigma^3=1.1$. A comparison of these data with those at $\rho\sigma^3=0.526$ [Figs. 4(a) and 4(b)] shows that while all the $g_{l,m}(r)$ become larger in amplitude and their peaks become narrower at the highest density, there are four which have undergone qualitative changes. These are $g_{4,0}$, $g_{4,4}$, $g_{6,0}$, and $g_{6,6}$. We noted in Sec. III that the pair correlation function $g(r)$ also shows new structure at this high density. Perhaps the most striking feature of this structure is the appearance of a new maximum which splits the first minimum of $g(r)$ into a double minimum. This occurs at $r=1.5\sigma$. The four functions $g_{4,0}$, $g_{4,4}$, $g_{6,0}$, and $g_{6,6}$ all show similar structure. In this respect they mimic the behavior of $g(r)$. It is interesting to recall that these four order parameters showed little change as the system froze. They showed the same behavior in the low density solid as in the dense fluid. However, when the solid is compressed, they change significantly and show much more structure. In this respect they are again mimicking the behavior of $g(r)$. We now show the relevant comparisons in more detail.

Figure 10 shows $g_{4,0}$ at the three solid densities and the metastable fluid while Fig. 11 shows the same comparisons for $g_{4,4}$. Clearly both order parameters show new structure at the high density. These changes in structure

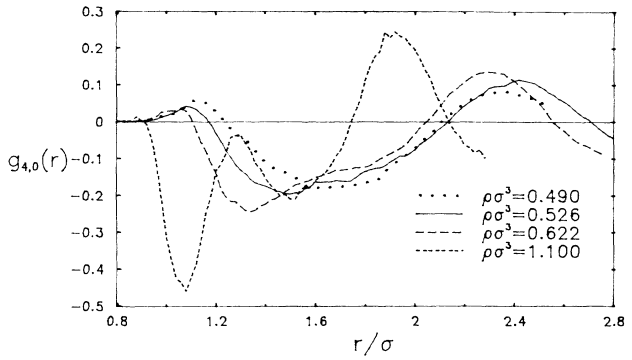

FIG. 10. Evolution in the behavior of $g_{4,0}(r)$ from a quantum metastable fluid, $\rho\sigma^3=0.490$ to a quantum solid, $\rho\sigma^3=0.526$ and 0.622, and finally, to an approximately harmonic solid at $\rho\sigma^3=1.10$.

are to be contrasted with the very small changes that take place in $g_{4,0}$ or $g_{4,4}$ as the system freezes. Figures 10 and 11 show very clearly how little these functions change as we pass from the high-density metastable fluid to the low-density solid.

Figures 12 and 13 show the same comparisons for $g_{6,0}$ and $g_{6,6}$. Again much more structure is present at the high density. In particular both functions show a double minimum between $r=1.5\sigma$ and $r=2.0\sigma$. The broad shoulder on $g_{6,6}$ at $r=1.5\sigma$, is absent at $\rho\sigma^3=1.1$. Again neither $g_{6,0}$ or $g_{6,6}$ show any significant changes as we pass from the fluid to solid phases.

We can summarize these comparisons in the solid phase by saying that in the high-density ^{4}He solid, which is approximately harmonic, the four angular order parameters $g_{4,0}$, $g_{4,4}$, $g_{6,0}$, and $g_{6,6}$ are distinctly different from the low-density solid. By contrast, the same order parameters are very similar in the low-density solid and high-density fluid up to 1.5σ. We have every reason to expect that the angular order parameters will all decay to zero at large r in the fluid phase. However in the solid phase we expect that they will display finite-amplitude oscillations at large r. This, as with $h(r)$, reflects the long range spatial order in the quantum solid.

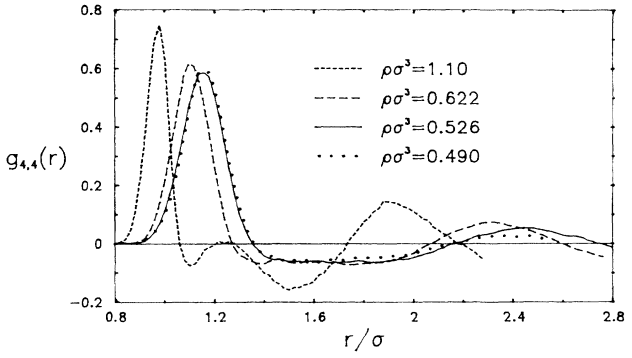

FIG. 11. Evolution in the behavior of $g_{4,4}(r)$ as the density increases from that of a quantum fluid to that of an approximately harmonic solid.

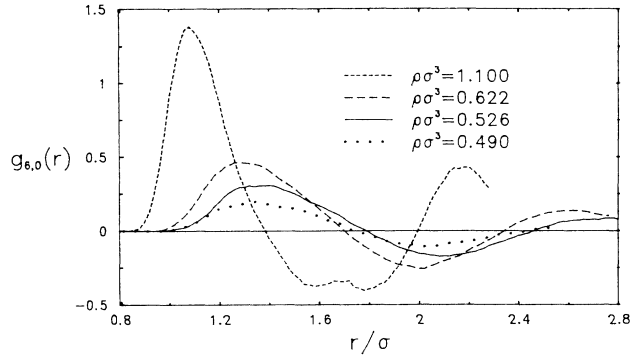

FIG. 12. Comparison of the behavior of the angular order parameter $g_{6,0}(r)$ as the density is increased from a quantum fluid to a nearly harmonic solid.

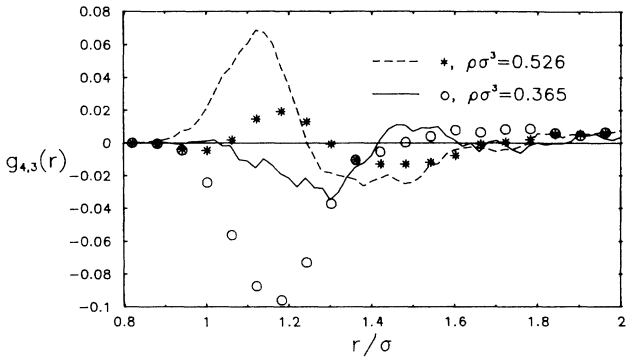

FIG. 14. Angular order parameter $g_{4,3}(r)$ from exact (GFMC) and Jastrow variational calculations at two densities. The exact result for a fluid at $\rho\sigma^3=0.365$ is indicated by ——; the variational result at this density is represented by open circles (○). The exact result for a solid at $\rho\sigma^3=0.526$ is shown as a dashed line (— — —); the Jastrow variational result is shown as asterisks (*).

VI. ANGULAR ORDER DETERMINED FROM VARIATIONAL WAVE FUNCTIONS

The most commonly used variational wave function for fluid ^{4}He consists of a symmetric product of functions, each of which depends on the separation of a pair of particles. This is the so-called Jastrow function:

$$\psi_J = \prod_{\substack{i,j \\ (i<j)}} f(r_{ij}) \ .$$

Considerable effort has been devoted to finding the best form for the function $f(r)$. Several authors[13,14] have suggested that an improved function should contain three particle correlations,

$$\psi_{J+T} = \prod_{\substack{i,j \\ (i<j)}} f(r_{ij}) \prod_{\substack{i,j,l \\ (i<j<l)}} F(r_i,r_j,r_l) \ .$$

This new form is said to have both pair and triplet correlations. In the solid phase either of these trial functions is usually multipled by a product of Gaussians, each of which localizes one of the particles on a lattice site. Recent Monte Carlo variational calculations[15] have shown that the inclusion of triplet correlations lowers the variational energy significantly. However the inclusion of triplet correlations has not been shown to produce significant changes in other properties, such as the pair distribution function or the momentum distribution. We investigated the variational angular order parameters at two densities, the equilibrium density fluid, and the solid near melting. Our data show very clearly that when triplet correlations are included in the trial function the angular order parameters are within the errors and in nearly all cases indistinguishable from those obtained from the exact computations. On the other hand, there are very significant differences, for some of the order parameters, i.e., $g_{4,3}(r)$, $g_{6,2}(r)$ and $g_{6,5}(r)$, between the variational results from the Jastrow function and the exact results. At the two densities, the other Jastrow order parameters were in less good agreement than those obtained with triplet correlations. In general, the Jastrow order parameters were shifted to slightly smaller values of r.

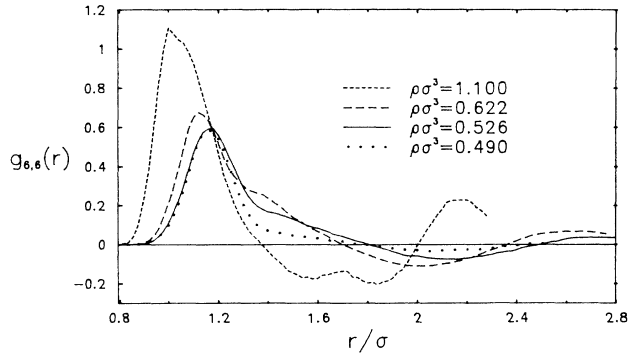

FIG. 13. Evolution in the behavior of the angular order parameter $g_{6,6}(r)$ as the density increases from that of a metastable quantum fluid to that of a nearly harmonic solid.

Figure 14 shows the comparisons of the Jastrow order parameters with the exact computations for $g_{4,3}$. In the solid phase the exact $g_{4,3}$ undergoes a complete oscillation between positive and negative values in the range $r=\sigma$ to $r=1.4\sigma$. This is to be contrasted with the results from the Jastrow function in which $g_{4,3}$ also oscillates but is very much smaller in amplitude. In the fluid phase the exact $g_{4,3}$ is small and negative from $r=\sigma$ to $r=1.6\sigma$, whereas the Jastrow $g_{4,3}$ shows a strong minimum in this range.

Figure 15 shows the comparisons for $g_{6,2}$. In the equilibrium fluid the exact $g_{6,2}$ remains close to zero for all r values, while $g_{6,2}$ computed from the Jastrow function shows a sizeable maximum between $r=\sigma$ and $r=1.6\sigma$. In the solid phase the exact $g_{6,2}$ shows a large amplitude oscillation between $r=\sigma$ and $r=1.8\sigma$. The variational calculation yields a $g_{6,2}$ that also oscillates in this region but with appreciably smaller amplitude. In Fig. 16 we show the same comparison for $g_{6,5}$. At the lowest density, the exact $g_{6,5}$ is close to zero for all values of r, while the variational result show a large minimum between

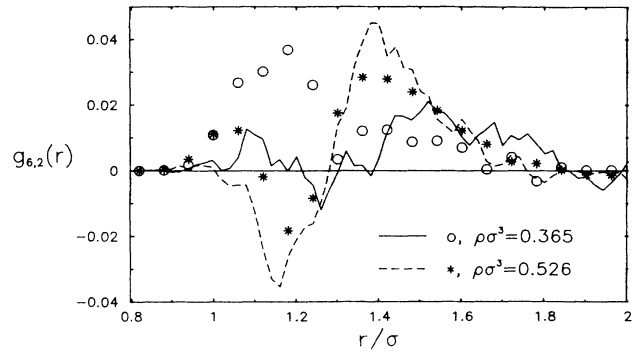

FIG. 15. Comparison of $g_{6,2}(r)$ from the exact computations with that from the Jastrow variational computations at two densities. The exact (GFMC) results for a fluid at $\rho\sigma^3=0.365$ are represented by a solid line (——) and the Jastrow results by open circles (○). For a solid at the density, $\rho\sigma^3=0.526$, the exact results are indicated by a dashed line (— — —) and the variational results are shown with asterisks (*).

$r=\sigma$ and $r=1.5\sigma$. In the crystal phase, the exact $g_{6,5}$ goes through a complete oscillation between $r=1.0\sigma$ and $r=1.7\sigma$. The variational result oscillates in a similar manner but with less amplitude.

It is interesting to note that the order parameters $g_{4,3}$, $g_{6,2}$, and $g_{6,5}$ calculated from a Jastrow function are in better agreement with the exact results in the solid phase than in the fluid phase. We believe that it is significant that of the angular order parameters that seem to signal the onset of freezing (cf. Sec. IV), $g_{4,3}$, $g_{6,2}$, and $g_{6,5}$ are qualitatively wrong when derived from a pure Jastrow trial function for the fluid.

VII. CONCLUSIONS

We can summarize our conclusions in the following way:

(i) The pair correlation functions $g(r)$ evolves smoothly from the lowest-density to the dense metastable fluid phase. No significant precursor to melting is evident. Upon freezing the short- and intermediate-range structure changes only slightly. The long-range behavior of $g(r)$ in the solid will, of course, reveal the presence of the long-range spatial order.

The pair correlation function in the solid phase shows a remarkably fluidlike structure. Only at an extremely high density of $\rho\sigma^3=1.1$ does the short- and intermediate-range order reflect the presence of the crystalline order. At this density, solid ^{4}He is approximately harmonic and $g(r)$ is very similar to the two-body correlation function in a classical solid just before melting. We conclude that, except for its long-range behavior, $g(r)$ provides very little information about the onset of freezing.

(ii) We have represented $g_3(r_{12},r_{13},r_{23})$ by a spherical harmonic expansion with respect to locally defined coordinates, which allows us to examine the angular order in the system. The interesting components of the expansion are $g_{4,m}(r)$ and $g_{6,m}(r)$. While none of these functions show a clear precursor to freezing, several of them undergo significant changes as the system solidifies. These are $g_{4,3}$, $g_{6,1}$, $g_{6,2}$, and $g_{6,5}$. The other $g_{l,m}(r)$ evolve smoothly until the high-density-solid phase is reached at $\rho\sigma^3=1.1$. At this density, several of these functions show the presence of crystalline order. We conclude that unlike $g(r)$, there are components of $g_3(r_{12},r_{13},r_{23})$, as represented by the $g_{l,m}(r)$, that change significantly on freezing. This suggests that these higher order correlations are important in the melting-freezing transition.

(iii) Some of these angular order parameters are sensitive to the structure of the variational functions that are often used in liquid and solid ^{4}He. When a Jastrow function is used to compute these functions $g_{4,3}$, $g_{6,2}$, and $g_{6,5}$ show significant discrepancies when compared with the exact GFMC results. However when triplet correlations are included in the wave function, the agreement with exact results is excellent for all the $g_{l,m}(r)$. We thus conclude that the inclusion of triplet correlations is necessary if the three-body correlations are to be correctly accounted for in a variational calculation. This is not surprising since the energy is known to be sensitive to three-body correlations. If the melting/freezing transition is dominated by three-body correlations, a good $(J+T)$ wave function may be sufficient to describe the transition.

(iv) Those $g_{l,m}(r)$ that do not change significantly when the system freezes evolve as the solid is compressed, and at the highest density at which we worked they show the presence of local crystalline order. This behavior mimicks that of $g(r)$.

We view this presentation and analysis of the behavior of the triplet correlations in liquid and solid ^{4}He as a preliminary attempt to understand the qualitative microstructure of these systems.

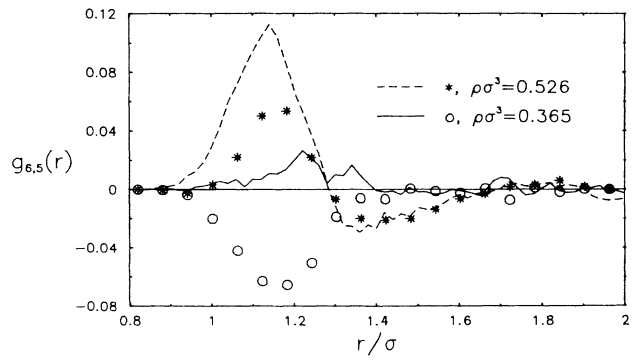

FIG. 16. Exact (GFMC) and Jastrow variational calculations of $g_{6,5}(r)$ compared at two densities. The solid line (——) represents the exact results for a fluid at $\rho\sigma^3=0.365$ and the open circles (○) the Jastrow results. The dashed line (— — —) shows the exact results for a solid at $\rho\sigma^3=0.526$ and the asterisks (*) are the variational results.

ACKNOWLEDGMENTS

It is a pleasure to acknowledge the helpful discussions we had with Dr. George O. Williams in the early stages of this project. He suggested the basic method of analysis and provided us with a copy of his code with which to

carry out the necessary computations. We also acknowledge the many helpful discussions with Luciano Reatto, Kevin Schmidt, Joseph Carlson, and Malvin Kalos. This work was supported by the National Science Foundation under Grant No. DMR-8513300 and by the Applied Mathematical subprogram of the Office of Energy Research, U. S. Department of Energy, under Contract No. DE-AC-02-76ER03077.

[1]B. J. Alder, and T. E. Wainwright, J. Chem. Phys. **27**, 1208 (1957); W. W. Wood, and F. R. Parker, J. Chem Phys. **27**, 720 (1957); W. G. Hoover, and F. H. Ree, J. Chem. Phys. **49**, 3609 (1968).

[2]J. P. Hansen, and I. R. McDonald, *Theory of Simple Liquids* (Academic, New York, 1970), Chap. 10.

[3]J. P. Hansen, and L. Verlet, Phys. Rev. **84**, 151 (1969).

[4]N. S. Gingrich and C. W. Thompson, J. Chem. Phys. **36**, 2398 (1962).

[5]H. R. Glyde, in *Rare Gas Solids,* edited by M. L. Klein and J. A. Venables, (Acadmic, New York, 1976), Chap. 7.

[6]P. A. Whitlock, M. H. Kalos, G. V. Chester, and D. M. Ceperley, Phys. Rev. B **21**, 999 (1980).

[7]The basic methodology we have used in liquid and solid ^{4}He was suggested to us by Dr. George Williams.

[8]For another method used in the analysis of classical systems, see P. J. Steinhardt, D. R. Nelson, and M. Ronchetti, Phys. Rev. Lett. **47**, 1297 (1981); Phys. Rev. B **28**, 784 (1983).

[9]The angular correlations computed by P. J. Steinhardt, D. R. Nelson, and M. Ronchetti, Ref. 8, are measured with respect to an external set of axes. Ours are measured with respect to a local set of axes set up for each particle in the system.

[10]For the Lennard-Jones potential, the melting and freezing densities are $\rho\sigma^3=0.48\pm0.01$ and $\rho\sigma^3=0.52\pm0.01$, respectively.

[11]G. Williams (private communication). The function $h(r)$ in a classical Lennard-Jones solid just before melting is remarkably close to that of $h(r)$ in solid helium at the reduced density $\rho\sigma^3=1.1$.

[12]L. Verlet, Phys. Rev. **165**, 201 (1968).

[13]C.-W. Woo, Phys. Rev. Lett. **28**, 1442 (1972); C.-W. Woo and R. L. Coldwell, *ibid.* **29**, 1062 (1972).

[14]C. C. Chang and C. E. Campbell, Phys. Rev. B **15**, 4238 (1977); V. R. Pandharipande, **18**, 218 (1978).

[15]K. E. Schmidt, M. H. Kalos, M. A. Lee, and G. V. Chester, Phys. Rev. Lett. **45**, 573 (1980); K. E. Schmidt, M. A. Lee, M. H. Kalos, and G. V. Chester, *ibid.* **47**, 807 (1981).